JOURNAL OF MATERIALS SCIENCE **37** (2002) 3381 – 3387

The production of ultrafine zirconium oxide powders by spray pyrolysis

W. NIMMO*, D. HIND, N. J. ALI, E. HAMPARTSOUMIAN, S. J. MILNE
School of Process, Environmental and Materials Engineering, The University of Leeds, UK
E-mail: w.nimmo@leeds.ac.uk

Twin-fluid atomisation spray-pyrolysis has been investigated for the production of ZrO_2 powders. The atomiser used in this study has a novel internal arrangement that can produce a spray with a mean diameter (SMD) of less than 5 μm. Spray pyrolysis tests with zirconium nitrate as a precursor salt were performed and the formation of ZrO_2 powder was studied under substantially different heating rates and initial solution concentrations. A mean particle diameter, $d(0.5)$, of 0.67 μm and 0.77 μm was achieved for 0.05 M and 0.5 M solutions, respectively. It was concluded that the new nozzle design performed well and was successful in producing ultra-fine ZrO_2 powder with a principally tetragonal structure when the correct process conditions of heating rate and residence time were applied.

1. Introduction

Various techniques [1–6] such as sol-gel, hydrothermal and spray-pyrolysis (SP) have been studied for producing ultrafine, electroceramic powders, for example, sol-gel, hydrothermal and spray-pyrolysis (SP). It is recognised [7] that the availability, on a cost effective basis, of micron and submicron powders in thick film processing would help satisfy the requirement to reduce the thickness of the ceramic layer to less than 10 microns. In principle, pressure-atomisation spray pyrolysis, provides a promising, but as yet unproven, route for producing chemically homogeneous ultrafine particles in the large quantities required for the commercial manufacture of electro-ceramic thick film devices. SP involves the formation of an aerosol of a precursor metal salt solution, which is passed through a graded temperature reactor in which the individual droplets are thermally decomposed to form oxide particles. Refinement of the process could offer potential advantages [8–12], in terms of particle homogeneity, over other production methods.

High capacity pressure spray atomisation [9] routes, for example, the Ruthner process, have been used for ferrite, mullite and cordierite powder production but because of the large droplet sizes that are produced in conventional pressure jet systems, after shrinkage, the particles were typically of the order of 25–100 μm in diameter [8]. Moreover, hollow spherical particles may form during pyrolysis due to poor control of evaporation rates and salt solubility resulting in excessive solute concentration at the surface of the droplets. This leads to premature surface precipitation and the formation of a low permeability surface skin at a very early stage of evaporation. Further shrinkage is then restricted giving rise to oversize hollow particles, partial fragmentation occurs due to the build up of pressure within the core of the particle to give a physically inhomogeneous product. Inevitably milling has to be used to breakdown the SP particles and produce a finer, more sinter-active ceramic starting powder [8].

At the research level the issue of reducing droplet/particle size has been addressed by replacing pressure sprays by ultrasonic atomisation techniques. The size of the droplets are principally dependant on the applied frequency, and micron scale droplets can be formed, but at low liquid flows of a few millilitres per minute [10]. Because of the compositional complexity of high T_c superconducting ceramics, ultrasonic SP has proved to be a popular means of preparing small quantities of powder [11], and has also been used to prepare a wide range of single and other multicomponent powders with sub micron particle sizes [8]. Using a twin fluid, air assisted atomiser, Messing *et al.* [8, 12] produced ZrO_2 powders and demonstrated that for 0.05 M salt solutions in combination with a low temperature pre-treatment to induce slow evaporation, it was possible to develop a route that avoided the steep solute concentration gradients that induce premature salt precipitation at the surface of the droplet during the early stages of shrinkage. Consequently, the formation of oversize hollow particles could be avoided. Particle diameters of 1 to 3 μm were obtained.

The work presented here represents the first results from a new SP installation, which incorporates a novel design of twin-fluid atomiser with a droplet classsification system and good control over furnace temperature profile.

*Author to whom all correspondence should be addressed.

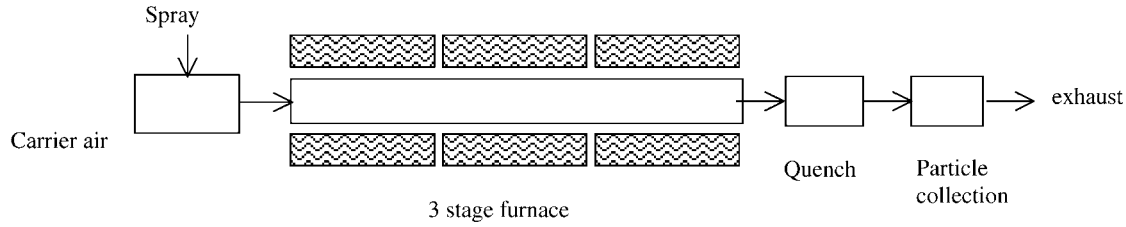

Figure 1 Schematic diagram of particle flow reactor used for spray pyrolysis.

2. Experimental equipment and method

A schematic diagram of the spray pyrolysis (SP) flow reactor is shown in Fig. 1 and consisted of 6 heated sections (maximum rating, 7 kW) which were linked to provide three independently controllable temperature zones. The overall length of the reactor was 2.5 m with an internal diameter of 70 mm. This reactor was used to generate a relatively gentle temperature gradient for droplet evaporation and salt precipitation prior to calcination.

The atomiser used for the experiments was designed in-house [13] and is a development of a twin-fluid design with internal mixing of gas and liquid. The new design (Fig. 2) induced a degree of pre-filming on the internal cone surface prior to ejection through the nozzle orifice producing a spray with a smaller mean droplet diameter than conventional effervescent atomisers [14, 15]. The size distribution of the spray was further modified by classification in a pre-chamber prior to entering the reactor. A constant pressure feed system was used (Fig. 3) to ensure a steady flow of solution to the nozzle of about 15 ml/min. Atomising air was fed at a rate of about 8 l/min.

Powders were collected from the reactor after an overall residence time of about 4 s in the SP reactor by knock out vessels and PTFE filters. X-ray diffraction analysis was performed on a Phillip APD 1700 diffractometer using Cu K_α radiation of wavelength 1.54050 A. Particle morphology and composition were studied using a Hitachi S700 for imaging (SEM) and a Camscan Series 4 with energy dispersive X-ray analysis (EDX) capabilities.

Spray-droplet and particle sizing was performed by the laser diffraction method using Malvern Mastersizer instruments.

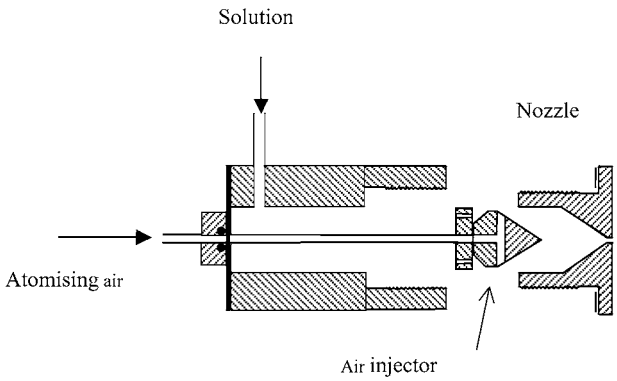

Figure 2 Schematic diagram of twin-fluid atomiser (unassembled).

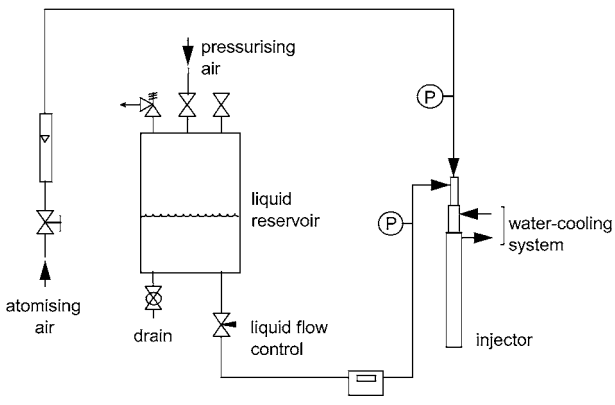

Figure 3 Low pressure injection system for air and liquid feed to the twin fluid atomiser.

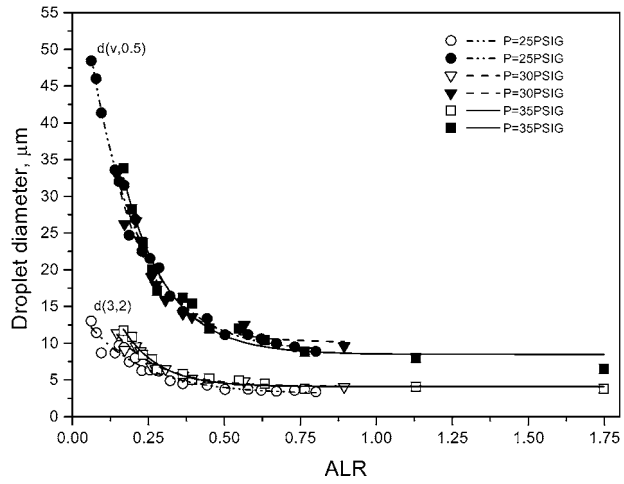

Figure 4 The effect of air/liquid mass ratio (ALR) on droplet size at 25, 30 and 35 psig.

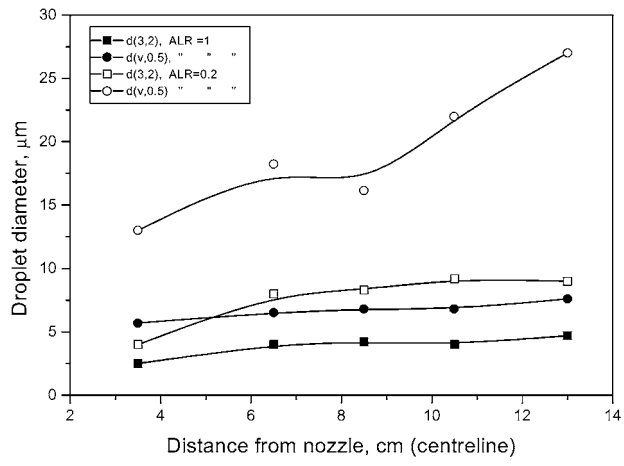

Figure 5 The variation of droplet diameter with distance from the nozzle.

3. Results and discussion

3.1. Droplet characterisation

Before pyrolysis experiments were performed, the atomiser droplet size was characterised using pure water over a range of air-liquid ratios (ALR's). Mean droplet sizes, $d(3,2)$ (Sauter Mean Diameter) and $d(v,0.5)$ are shown in (Fig. 4). Reduction in droplet size is observed at higher ALR and is typical of the response of twin fluid atomisers. At an ALR of 1 droplet sizes $d(v,0.5)$, and $d(3,2)$ of 9 μm and 4 μm, respectively, are obtained with 90% of the droplets having diameters less than 17 μm ($d(v,0.9)$). The results indicate that there is only a marginal improvement in droplet size when the atomisation pressure is increased from 25 psig to 35 psig however there are significant gains in liquid throughput. For example, it was found that at an air mass flow rate of 7 g/min, an increase in the liquid mass flow rate from 15 g/min to about 32 g/min is achieved; an increase of over 100%. This is an important factor in the design of a spray-pyrolysis process where the throughput of the system can be increased significantly with no significant reduction in spray quality. The droplet size ($d(3,2)$) could be maintained below 5 μm for liquid mass flow rates up to about 20 g/min at 35 psig and 17 g/min at 25 psig. The variation of droplet size along the axis of the spray is shown in Fig. 5. At a pressure of 30 psig and an air flow rate of 8 l/min (ALR = 1) only a slight increase in droplet size is observed beyond about 6 cm from the atomiser indicating that there is only a little coalescence due to droplet collision and is the case for both $d(3,2)$ and $d(v,0.5)$. At the lower air input of 5.6 l/min (ALR = 0.26) significantly more coalescence is observed, probably due to the higher droplet density in this spray and the increased likelihood of droplet collisions. An example of the droplet size distribution from the atomiser is shown in Fig. 6 (at 25 psig). A spray with an SMD of about 3.5 μm was obtained by operating the atomiser at an ALR of 1.

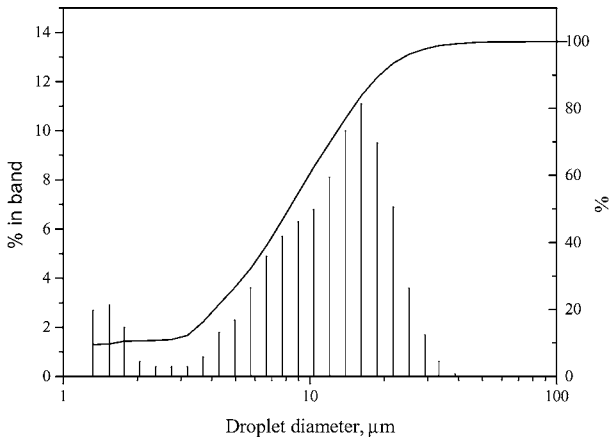

Figure 6 Size distribution of droplets at a distance of 10 cm from nozzle (25 psi).

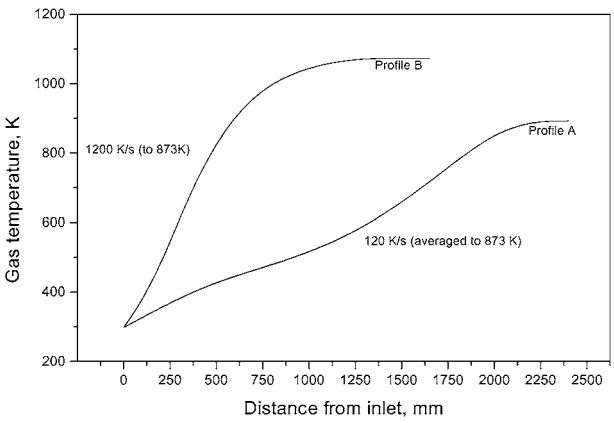

Figure 7 Gas temperature profiles during ZrO_2 production. Profile A—gradual heating 120 K/s. Profile B rapid heating 1200 K/s.

3.2. Particle morphology

The gas temperature profiles in the SP reactor (Profile A) and the DTR reactor (Profile B) are shown in Fig. 7. The heating rates to 873 K of 120 K/s and 1200 K/s were chosen for comparison due to their significant difference which would serve to demonstrate the effect of heating rate on particle morphology. We

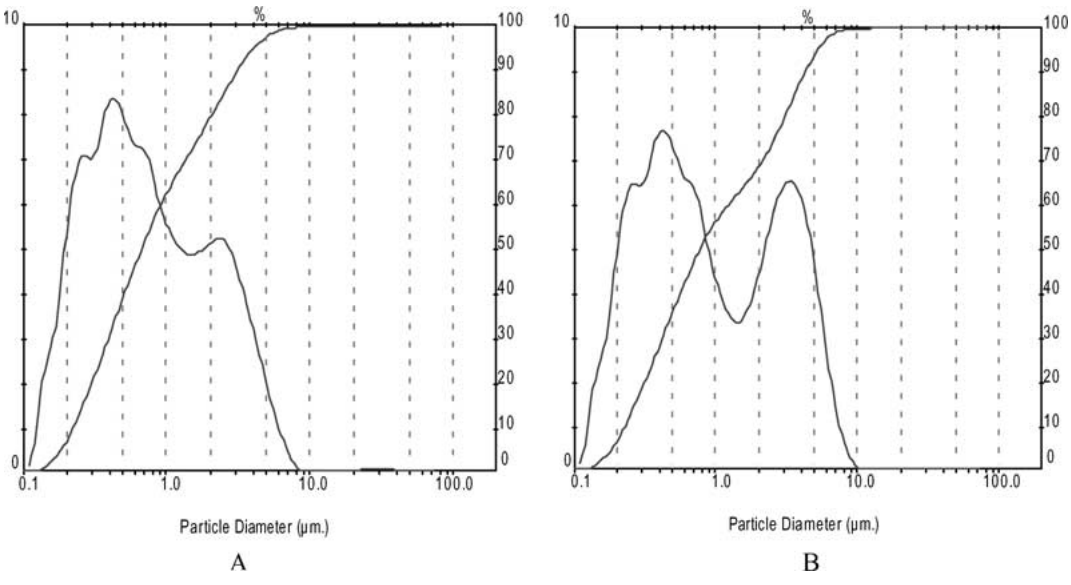

Figure 8 ZrO_2 particle size distribution for initial solution concentrations of A—0.05 M and B—0.5 M.

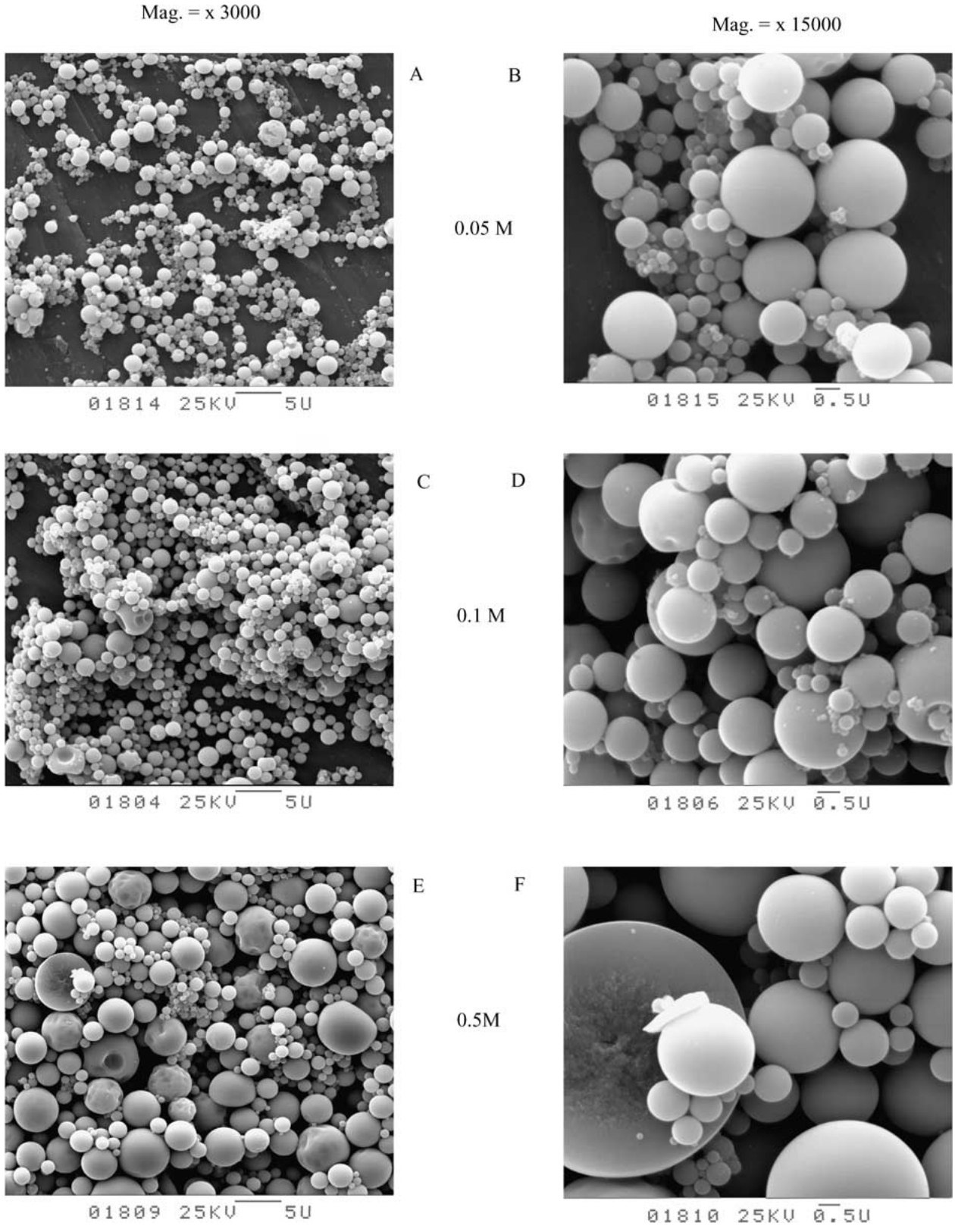

Figure 9 SEM image of sub-micron particles formed from 0.05, 0.1 and 0.5 M zirconium nitrate solution in the spray pyrolysis flow reactor.

cannot assume that the droplet/particle will follow the gas temperature precisely, due to heat and mass transfer considerations [16]. Nevertheless, the gas temperature profiles shown in Fig. 7 are valid representations of the process conditions experienced by the aerosol as it progresses through the reactors.

The size distribution of the ZrO_2 particles formed in the SP reactor are shown in Fig. 8 for initial solution concentrations of 0.05 M and 0.5 M. Both distributions show a bi-modal character with peaks at 0.3 μm and 3 μm but the latter peak more intense for the 0.5 M solution. This is reflected in the statistical analysis of the size distributions (Table I) and in particular the $d(v, 0.9)$ value which is 3.1 μm for the weaker solution and 4.2 μm for the more concentrated solution.

The bi-modal distribution is visually apparent under in SEM micrographs (Fig. 9) for precursor solution concentrations of 0.05, 0.1 and 0.5 M. The approximate, observed size ranges were 0.25–2.5 μm, 0.3–4 μm and 0.5–6 μm respectively. Fractured particles (Fig. 9E and F) confirm the fully dense structure of the spherical particles and are proof of volumetric salt precipitation in the droplets. There are, however, some irregularly shaped particles with surface indentation, which may be evidence for cavities in some of the particles. There is a slight increase in the observed particle size when the concentration of the precursor zirconium nitrate solution is increased from 0.05 M to 0.1 M which may be explained by the calculation of the theoretical particle size after liquid evaporation using [8],

$$D_p = D_0\left(\frac{C_0}{C_s}\right)^{\frac{1}{3}}\left(\frac{\rho_{\text{salt}}W}{\rho_{\text{oxide}}(1-P)}\right)^{\frac{1}{3}} \qquad (1)$$

TABLE I ZrO_2 particle size statistics

	Diam. (μm) (0.05 M)	Diam. (μm) (0.5 M)
$D(v, 0.5)$	0.67	0.77
$D(v, 0.1)$	0.27	0.23
$D(v, 0.9)$	3.1	4.23
Mode	0.42	0.42

D_0 = starting droplet diameter μm, C_0 = starting droplet concentration, C_s = saturation droplet concentration ρ_{salt}, ρ_{oxide} = density of salt and oxide phases, W = oxide yield of salt(s), P = fractional porosity of the particle where volumetric precipitation is assumed. For example, a 5 μm droplet of 0.05 M and 0.1 M concentration is calculated to form a 1.2 μm and 1.47 μm particle, respectively and gives a size ratio 1.26 for the given change in initial concentration. However, for a 10-fold increase (0.05 M to 0.5 M) the application of Equation 1 gives a ratio of 2.2, that is the particle diameter is more than doubled as can be seen by comparing Fig. 9C and E.

In contrast, the SEM images of zirconia particles from the DTR at the higher heating rate (Fig. 10) show evidence of surface precipitation of salt on heating followed by the formation of a shell which may break up explosively by the release of internal pressure. This type of behaviour leads to secondary atomisation of the droplets and the formation of smaller sub-micron particles. The majority of these particles appear to be complete, spherical and solidly formed. This may lead to the conclusion that even at concentrations close to saturation (i.e. 0.5 M) the small diameter particles have a tendency for volumetric precipitation rather than the surface precipitation of the larger particles due to shorter diffusion distances. For volumetric precipitation to occur, the concentration at the centre of the droplet must

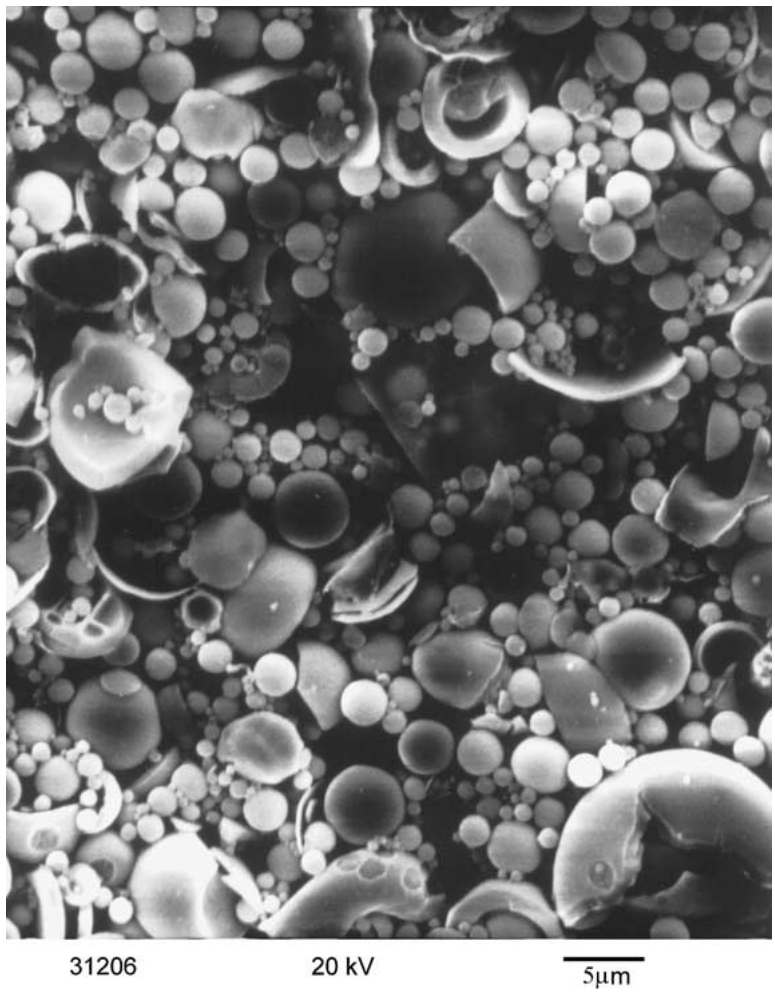

Figure 10 SEM image of sub-micron particles formed from 0.5 M zirconium nitrate solution in drop tube rapid pyrolysis reactor.

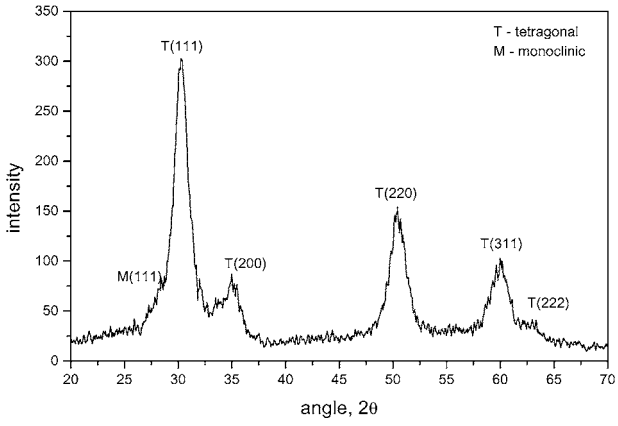

Figure 11 XRD pattern of ZrO_2 prepared by SP at $T_{max} = 600°C$.

be greater than or equal to saturation at the droplet temperature. If volumetric precipitation has occurred in the droplets then the development of concentration gradients may have been minimised by internal mixing of the solution by convection. Therein lies the key to the formation of ideal solid particles, by controlling the relative rates of droplet shrinkage and concentration redistribution within the droplet. This is achieved by creating the appropriate gas temperature profile as demonstrated in the SP reactor.

The use of precursor salt solutions other than nitrates, for example acetates, has shown that the formation of hollow shells can be avoided [8, 17, 18]. However, under certain circumstances, due to the formation of an intermediate gel-like phase during particle formation, dimpled morphology can occur in particles greater than 3 μm. These undesirable structures can be avoided by the careful control of the droplet/particle heating rates that are experienced inside the spray pyrolysis furnace [17].

XRD patterns of the powders from the SP reactor (Fig. 11) were compared with the standard JCPDS patterns for the tetragonal, monoclinic and cubic phases [19]. The dominant phase in the ZrO_2 from SP was found to be tetragonal with a slight indication of a monoclinic phase. Previous work indicates that, due to crystallite size effects principally tetragonal phase is expected [8] from SP synthesis of zirconia although a mixture of tetragonal and monoclinic has been observed in zirconia produced from flame-assisted ultrasonic spray pyrolysis [20].

Having established operating conditions for one nozzle and, although the subject of future work, one can see how the scale-up of the process could be achieved using multi-nozzle arrays. However, there are potential problems. The interaction between individual spray cones [21–23] in a multi-nozzle system and the subsequent droplet coalescence that would inevitably occur, would need to be minimised by careful spray chamber design. The number of nozzles, which constitutes an optimum arrangement, could be determined experimentally. Further process design considerations include furnace diameter, length and particle residence time. The heat required by the process would be determined by heat balance calculation, with the heat required for water evaporation being a major consideration. Furnace temperature profile and particle temperature history, are other important considerations with direct influence on powder quality. Process design may also be aided by the use of mathematical models of the spray-pyrolysis process [16, 24, 25] which describe droplet evaporation and solid particle formation.

4. Conclusions

ZrO_2 powder has been prepared by twin-fluid atomisation. The atomiser has a novel internal arrangement, which can produce a spray with mean diameter (SMD) of less than 5 μm representing a good initial droplet size for solid particle formation by spray-pyrolysis. Further classification of the spray removed the oversize droplets greater than 10 μm.

Experiments with a model ceramic precursor salt ($Zr(NO_3)_2$) have shown that dilute solutions (0.05 M) can produce solid, spherical ZrO_2 with mean particle diameter, $d(0.5)$, of 0.67 μm indicating that volumetric solids precipitation predominates during particle formation.

At concentrations approaching saturation (0.5 M), under rapid heating, the process of particle formation is affected by, surface precipitation and the formation of hollow shells that may burst violently, releasing the liquid contents in a secondary atomisation process.

Acknowledgements

We are grateful to the UK EPSRC for financial support for this work, Mr. Raymond Cowling for assistance in the design and construction of the twin-fluid atomisers and Mr. Paul Barton for assistance with spray characterisation.

References

1. D. HIND and P. KNOTT, In "Electroceramics," edited by W. E. Lee and A. Bell (Inst. of Materials, 1994) p. 107.
2. H-W. WANG, D. A. HALL and F. R. SALE, *J. Amer. Ceram. Soc.* **75** (1992) 124.
3. A. P. SINGH, S. K. MISHRA, D. PANDEY, C. D. PRASAD and R. LAL, *J. Mater. Sci.* **28** (1993) 5050.
4. H. HIRASHIMA, E. ONISHI and M NAKAGAWA, *J. Non-Cryst. Solids* **121** (1990) 404.
5. M. M. LENCKA, A. ANDERKO and R. E. RIMAN, *J. Amer. Ceram. Soc.* **78** (1995) 2609.
6. D. CHEN, X. JIAO and R. XU, *J. Mater. Sci.* **17** (1998) 53.
7. S. L. SCHWARTZ, T. R. SHROUT and T. TAKENAKA, *Bull. Am. Cer. Soc.* **76** (1997) 51.
8. G. L. MESSING, S-C. ZHANG and G. V. JAYANTHI, *J. Amer. Ceram. Soc.* **76** (1993) 2707.
9. M. J. RUTHNER, In "Ceramic Powders," edited by P. Vincenzini (Elsevier, 1983) p. 15.
10. D. J. JANACKOVIC, V. JOKANOVIC, L. J. KOSTIC-GVOZDENOVIC, L. J. ZIVKOVIC and D. USKOKOVIC, *J. Mat. Res.* **11** (1996) 1706.
11. C. H. CHAO and P. D. OWNBY, *J. Mater. Sci.* **30** (1995) 6136.
12. S-C. ZHANG and G. L. MESSING, *J. Amer. Ceram. Soc.* **73** (1990) 61.
13. W. NIMMO, J. AGNEW, E. HAMPARTSOUMIAN and J. M. JONES, *Industrial and Engineering Chemistry Research* **38** (1999) 2954.
14. J. S. CHIN and A. H. LEFEBVRE, *J. Engineering for Gas Turbines and Power* **117** (1995) 266.

15. S. D. SOVANI, P. E. SOJKA and A. H. LEFEBVRE, *Progress in Energy and Combustion Science* **27** (2001) 483.
16. Y. XIONG and T. T. KODAS, *J. Aerosol Sci.* **7** (1993) 893.
17. W. NIMMO, N. J. ALI, R. BRYDSON, C. CALVERT, E. HAMPARTSOUMIAN, D. HIND and S. J. MILNE, *J. Amer. Ceram. Soc*, submitted.
18. X. ZHAO, B. ZHENG, H. GU, C. LI, S. C. ZHANG and P. D. OWNBY, *J. Mat. Res.* **14**(7) (1999) 3073.
19. X-ray powder diffraction files for ZrO_2, JCPDS-tetragonal (17-923, 42-1164); monoclinic (13-307); cubic (30-1468, 26-341).
20. F. L. YUAN, C. H. CHEN, E. M. KELDER and J. SCHOONMAN, *Solid State Ionics* **109** (1998) 119.
21. G. BRENN, F. DURST and A. SELBERGH, *Particle and Particle Systems Characterisation* **15**(6) (1998) 263.
22. Y. HARDALUPAS and J. H. WHITELAW, *Journal of Fluids Engineering-Transactions of the ASME*, **118**(4) (1996) 762.
23. D. H. CHARLESWORTH and W. R. MARSHALL, *AIChE Journal* **6**(1) (1960) 9.
24. H.-F. YU, *Part. Sci and Tech.* **13** (1995) 149.
25. I. W. LENGGORO, T. HATA, F. ISKANDAR, M. L. LUNDEN and K. OKUYAMA, *J. Mat. Res.* **15**(3) (2000) 733.

Received 6 November 2001
and accepted 17 April 2002